2025 IMEKO TC-6 International Conference on
Metrology and Digital Transformation - **M4DConf 2025**
Benevento, Italy, September 3-5, 2025

Quantum Channel Characterization in QKD: A Metrological Perspective

Fatemeh Khalesi[1], Ioan Tudosa[1], Francesco Picariello[2], Arman Neyestani[1], Sergio Rapuano[1*]

[1]*Department of Engineering, University of Sannio, Benevento, Italy*
[2]*Department of Engineering and Science, Mercatorum University, Rome, Italy*
f.khalesi@studenti.unisannio.it, {ioan.tudosa, neyestani, rapuano}@unisannio.it, francesco.picariello@unimercatorum.it

***Abstract* – Quantum Key Distribution (QKD) offers secure communication by leveraging core principles of quantum mechanics. Characterization of QKD system is fundamental for comparing the experimental results provided by researchers. Unfortunately, there is no standardized or unified approach; therefore, different researchers present results that provide heterogeneous information, making comparisons difficult. A systematic analysis of the literature is necessary to identify common approaches from a metrological perspective. This paper provides an overview of measurements used to characterize quantum channels, with a focus on parameters such as attenuation, polarization effects, and timing stability. To support this analysis, real-world case studies are examined.**

Keywords: Quantum Channel, QKD, Metrological Characterization.

I. INTRODUCTION

Quantum Key Distribution (QKD) is a cryptographic technique that leverages quantum mechanics to securely generate and share encryption keys between two parties. Unlike classical cryptography, which relies on computational complexity, QKD offers *information-theoretic security* by encoding information in quantum states—typically modifying properties of single photons transmitted over optical links [1]. The emergence of quantum computing poses a significant threat to classical cryptographic systems, as quantum algorithms like Shor's and Grover's can efficiently break commonly used classical encryption schemes [2]. In contrast, QKD remains secure even in the presence of quantum adversaries [1]. Security is guaranteed by quantum principles: the *Heisenberg indeterminacy principle* prevents the precise simultaneous measurement of conjugate variables, while the *no-cloning theorem* prohibits copying unknown quantum states [2, 3].

Practical QKD systems are intrinsically affected by environmental noise, signal attenuation, and decoherence within quantum channels [3]. While most QKD implementations emphasize system design and functional performance, the thorough characterization of quantum channels—particularly incorporating principles such as traceability, repeatability, and reproducibility—is often overlooked [4]. This study investigates how quantum channel parameters influence key metrological aspects of QKD systems. It provides a review of current characterization approaches and analyzes real-world case studies to identify benefits, challenges, and gaps in practice. The focus is on how improved quantum channel characterization can enhance core measurement attributes such as accuracy, repeatability, reproducibility, and traceability, with attention to emerging needs for standardization.

To support this objective, Section II introduces a typical QKD system. Section III presents the metrological characterization of quantum channels, while Section IV provides supporting real-world case studies. Section V offers a comparative analysis and highlights research gaps and future directions. Finally, Section VI concludes the study.

II. QKD SYSTEM OVERVIEW

The process of QKD between Alice (Sender) and Bob (Receiver) is illustrated in Fig. 1, in which a secure key is shared using a quantum channel to transmit qubits—or optionally, entangled qubits—and a separate classical channel to perform basis reconciliation. A qubit is the basic unit of quantum computing, like a classical bit but able to exist in a superposition—being both 0 and 1 at once. Qubits can also be entangled, meaning the state of one instantly influences another, even at a distance. These properties allow detection of eavesdropping due to the delicate nature of quantum states [5].

To begin, Alice encodes single photons or photon pairs in a chosen quantum basis and sends them through the fiber to Bob. Optical loss during transmission in the fiber critically impacts QKD performance and is measured using standard tools such as an Optical Power Meter (OPM), which assesses input/output power to calculate loss during setup, and an Optical Time-Domain Reflectometer (OTDR), which locates loss points along the fiber but is used offline due to its high-intensity pulses [6, 7].

At Bob's side, sensitive Single-Photon Detectors (SPDs) register the incoming photons. Devices such as Superconducting Nanowire SPDs (SNSPDs) offer ultra-low jitter, high efficiency, and low dark counts, ideal for long-

*This work was supported by PNRR – Mission 4, Component 2, Investment 1.5 – ECS_00000024 – Rome Technopole – Call CODBAN_000378 – Spoke 3 – Project N. UR301-2023-000090 – "MES&QT: Distributed Measurement Systems based on Quantum Technologies for Secure Communications".

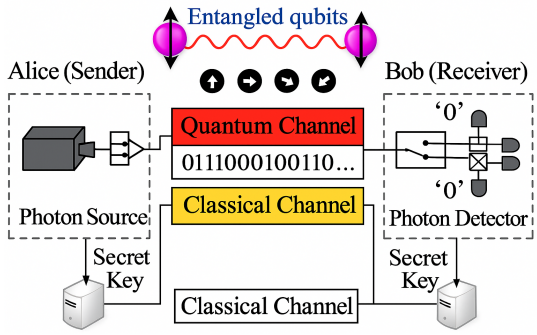

Fig. 1. A Schematic of QKD, qubits are transmitted over a quantum channel, while bits are exchanged via a classical channel for basis reconciliation and key verification [5].

distance QKD [8, 9], while Single-Photon Counting Modules (SPCMs) provide compact, integrated detection with built-in electronics [10]. Other similar detectors are also used depending on system requirements.

Timing synchronization is critical to ensure correct qubit detection. This is achieved using such tools as: (I) Time-to-Digital Converters (TDCs) and Time Interval Analyzers (TIAs) at Bob's side for high-precision timestamps [11, 12]; (II) GPS-Disciplined Oscillators (GPSDOs) and atomic clocks at both ends for stable long-term timing [13]; and (III) Phase-Locked Loops (PLLs) and frequency synthesizers embedded in hardware to generate and stabilize clock signals [9].

Finally, Alice and Bob perform basis reconciliation by comparing which bases they used— typically rectilinear ($|0\rangle, |1\rangle$) or diagonal ($|+\rangle, |-\rangle$). They keep only the bits where their bases match [5]. Then, in key verification, a subset of bits is compared to detect eavesdropping. If the quantum bit error rate (QBER) is below a set threshold, the rest of the bits are used to form a secure key [5].

III. QKD CHANNEL CHARACTERIZATION

Accurate quantum channel characterization is essential for optimizing QKD system performance and ensuring its security. This section reviews key channel parameters, the corresponding measurement methods, and the physical components involved in a quantum communication link. Although various methods are available, measurement uncertainty is rarely quantified or reported, which limits the reliability and comparability of results. The selected parameters are influenced by physical effects—such as absorption, thermal noise, mechanical stress, and signal jitter—that degrade signal integrity and contribute significantly to the overall uncertainty in QKD measurements.

A.1 Channel Attenuation (Optical Loss)

Photon loss in quantum communication channels primarily results from absorption, scattering, and imperfect coupling in optical fibers or free-space links [14, 15]. Attenuation refers to the reduction of signal strength during transmission and is typically expressed in *decibels per kilometer (dB/km)* and can be measured by devices like OPM or OTDR. It is defined as the ratio of output power (P_{out}) after transmission through a link of length L to the input power (P_{in}) [16]:

$$\text{Attenuation } \alpha = \frac{-10}{L} \log \left(\frac{P_{\text{out}}}{P_{\text{in}}} \right) \tag{1}$$

Attenuation reduces the number of detected photons, weakening the signal relative to background noise, and thereby increasing the QBER. The QBER is dimensionless and typically expressed as a percentage (%) and is calculated as [17]:

$$\text{QBER} = \frac{R_{\text{error}}}{R_{\text{error}} + R_{\text{sift}}} \tag{17}$$

where R_{error} is the rate of erroneous bits, and R_{sift} is the rate of sifted bits correctly received when basis choices match [17, 18].

The attenuation also directly affects the Secure Key Rate (SKR), R, which quantifies the number of secret key bits generated per second [19].

$$R = \nu \cdot s \cdot p \cdot q \cdot (d \cdot (1 - H(\text{QBER})) - f \cdot H(\text{QBER})) \tag{2}$$

where: ν is the *pulse repetition rate* (Hz), indicating how many light pulses (e.g., from a laser) are sent per second, set by the hardware, s is the *sifting coefficient*, the fraction of raw key bits retained after basis reconciliation (typically ≈ 0.5 for BB84, one of the possible QKD protocols), p is the *parameter estimation efficiency*, representing the portion of sifted bits used for key generation after estimating the QBER, q is the *transfer/measurement factor*, a dimensionless parameter reflecting losses in the quantum channel and detector inefficiency, d is the *decoy-state coefficient*, estimating the fraction of secure single-photon events via intensity-varying pulse analysis, f is the *error correction inefficiency*, quantifying the overhead beyond the Shannon limit during classical error correction, $H(\text{QBER})$ is the *binary Shannon entropy*, defined as $H(x) = -x \log_2 x - (1-x) \log_2 (1-x)$, measuring the information leakage due to errors in the key. QBER and SKR can be measured by devices like SPDs and SNSPDs.

In the characterization of QKD systems, measurement uncertainty is significantly influenced by channel attenuation. As attenuation increases, the photon detection rate decreases, which amplifies statistical fluctuations and raises the uncertainty in the QBER. These uncertainties have a direct effect on the SKR, since the SKR is highly sensitive to both detection efficiency and error rates.

A2. Dark Count Rate / Background Noise: A dark count is a false detection event in the absence of a photon, caused by thermal noise, electronic fluctuations, defects, or ambient light. The Dark Count Rate (DCR), measured in counts per second (cps), is evaluated by blocking the

input and counting false detections over a known time interval [20].

$$N_{0.5p.e}(T) \approx AT^{\frac{3}{2}} \exp\left(-\frac{E_g}{2kT}\right) \tag{3}$$

The detector measures the DCR N, defined at a 0.5 photoelectron threshold within the pulse window, and is temperature-dependent. The DCR can be modeled as a function of temperature T, where A is a constant related to charge trap formation during avalanche events, E_g is the semiconductor bandgap energy, and k is Boltzmann's constant [20].

To model the relationship between QBER and DCR [18]:

$$\mathrm{QBER} = \frac{R_{\mathrm{fACF}}}{R_{\mathrm{sift}} + R_{\mathrm{error}}} + \frac{R_{\mathrm{dc}}}{R_{\mathrm{sift}} + R_{\mathrm{error}}} \tag{4}$$

where R_{fACF}: error rate from frequency/polarization misalignment; R_{dc}: error rate due to dark counts ; R_{error}: total error detection rate ($= R_{\mathrm{fACF}} + R_{\mathrm{dc}}$). Lowering the DCR is key to keeping QBER low, especially over long distances or high loss. One of the devices that directly measures DCR and helps evaluate both QBER and SKR is the SPCM. Regarding measurement uncertainty, [21] reported a DCR uncertainty of 1% under stable conditions, combining Type A (0.1%) from Poisson statistics and Type B (0.9%) from temperature ($\pm 0.25\,^{\circ}\mathrm{C}$) and threshold variations.

A3. Polarization Drift: The gradual, often unpredictable change in an optical signal's polarization due to temperature, stress, or fiber bending, causing misalignment between sender and receiver, increases QBER, and reduces SKR. The polarization misalignment angle θ is estimated using the following formula [22]:

$$\theta \approx \arcsin\left(\sqrt{\frac{N_{\mathrm{erroneous}}}{N_{\mathrm{max}}}}\right) \tag{5}$$

where $N_{\mathrm{erroneous}}$ is the number of erroneous single-photon detections ($N_{\mathrm{erroneous}} = R_{\mathrm{error}} \cdot \Delta t$ in the measurement interval Δt), N_{max} is measured during calibration under ideal alignment and represents the maximum expected single-photon detections for a given intensity. It serves as a reference for estimating polarization misalignment.

In QKD systems, polarization drift is addressed by two separate devices with distinct functions: the *polarimeter* for measuring and the *Polarization Controller (PC)* for correction. The polarimeter measures the state of polarization (SOP) of incoming photons and detects deviations. Its output is used to estimate $N_{\mathrm{erroneous}}$. Then, the PC can actively adjusts the SOP.

Due to polarization drift, the measurement uncertainty observed in the paper [23] is approximately 2–3% in terms of QBER. This is considered a Type A uncertainty, as it is derived from statistical analysis of repeated experimental measurements over thousands of compensation cycles.

A4. Timing and Frequency Synchronization: Accurate synchronization is crucial in QKD to minimize QBER [24]. *Timing synchronization* ensures that Alice and Bob agree on when photons arrive. Optical clock pulses are sent at intervals ΔT_s, which are divided into N_w equal time windows of length τ_w [25]:

$$\Delta T_s = N_w \cdot \tau_w \tag{6}$$

This allows Bob to correctly identify photon arrival windows, minimizing errors (QBER) by aligning detection times with transmission. *Frequency synchronization* is achieved by locking to the pulse repetition rate $f = 1/\Delta T_s$. Precision instruments like TDCs and GPSDOs are used to ensure accurate synchronization. Time measurement uncertainty mainly comes from detector jitter and synchronization, typically ranging between 10 ps and 100 ps, as stated in [26]. Another study [27] reports a timing resolution of 12.6 ps (Type B) using a Field-Programmable Gate Array (FPGA) device, and a stability uncertainty of 8.4% (Type A), based on the standard deviation of the interference amplitude over time [27].

A.5 Environmental Effects: Changes in temperature, vibrations, and humidity increase uncertainty in QKD systems. These factors can disrupt alignment, detector efficiency, and timing, which leads to higher QBER and lower SKR [28]. To assess environmental impacts on quantum communication systems, a test chamber and various instruments can be used. (I) *Environmental Test Chambers* are used for offline lab testing to simulate controlled temperature and humidity variations, helping evaluate system stability under extreme conditions [29]. (II) *Accelerometers and Vibration Sensors* are deployed in both lab and field settings for real-time monitoring of mechanical disturbances that may affect optical alignment or system stability [30]. (III) *Fiber Bragg Grating Sensors* offer distributed, real-time measurements of strain and temperature along optical fibers, making them particularly suitable for field diagnostics [31]. (IV) *Infrared Thermometers and Thermocouples* provide continuous temperature readings of critical components, supporting both lab characterization and in-field operation [32].

IV. CASE STUDIES

This section summarizes four practical implementations of QKD. While much of the existing research focuses on designing and testing QKD systems, many papers lack key details needed to evaluate how reliable or accurate the results are.

A. Case Study 1: A Room-Temperature QKD System

The case study [33] presents a metrological evaluation of a room-temperature molecular single-photon QKD system in a free-space laboratory. Key quantum channel parameters were measured, with uncertainties interpreted based on experimental context. Channel loss was emulated

using up to 27 dB variable attenuators and quantified by measuring detector efficiency, reported as $30\% \pm 2\%$. This value was obtained through calibration with power meter measurements and spectral averaging, corresponding to a Type B uncertainty. The QBER was computed from photon detection statistics using single-photon avalanche detectors (SPADs), resulting in a value of $3.4\% \pm 0.2\%$ with Type A uncertainty based on statistical variation. The SKR was derived from the measured QBER and photon count rates, yielding up to 0.5 ± 0.05 Mbits/s in a back-to-back setup. This includes both Type A and Type B uncertainties. The DCR was extracted by fitting the QBER-loss relationship and was found to be in the range of 0.4 to 4×10^{-6} cps (Type A). Polarization drift was inferred from the detection error probability, which was $3.9\% \pm 0.5\%$ and reduced to 2.0% when a spectral bandpass filter was used. These effects are attributed to limitations in polarization control across a broadband emission spectrum, reflecting Type B uncertainty. The setup showed good repeatability under laboratory conditions and traceability through calibration-based measurements. Reproducibility was limited due to manual alignment and lack of environmental control. Despite these limitations, the study achieved a significant milestone by demonstrating a compact, room-temperature QKD system with performance comparable to cryogenic implementations [33].

B. Case Study 2: QKD Deployment Over 78 km Fiber

The paper [8] presents a QKD system over a 78 km fiber link between Braunschweig and Hannover, Germany. Entangled photon pairs were generated using a 532 nm laser via spontaneous parametric down-conversion in temperature-controlled ppKTP crystals, achieving entanglement fidelities of up to 95%. The signal photon is detected locally at Alice using a Single-Photon Avalanche Diode (SPAD)—a semiconductor detector sensitive to individual photons in the visible to near-infrared range. The idler photon travels through the fiber to Bob, where it is detected using an SNSPD that is ideal for telecom wavelengths [8]. The QKD system was characterized in both laboratory and field settings. Channel attenuation was measured using OTDR, revealing losses up to 29 dB over 78 km. QBER and SKR were derived from photon arrival times recorded by SPADs (Alice), SNSPD (Bob), and time taggers. SKR reached 1200 bps at 52 km and 30 bps at 102 km. Background photon counts of up to 5000 cps were observed due to crosstalk, mitigated by a 0.1 nm fibered bandpass filter. Polarization drift was compensated internally. From a metrological perspective, uncertainties arose from Raman noise (which is caused by scattered light from classical signals in optical fibers). The results were repeatable under laboratory conditions and reproducible when equivalent losses were introduced using long fiber spools or calibrated optical attenuators. While the spools simulated real-world transmission effects, the attenuators allowed for controlled testing without introducing additional fiber noise. Repeatability is supported by 24-hour performance averages and consistent trends in SKR and QBER. However, reproducibility remains only partially addressed, as no independent or cross-laboratory validation was conducted. Traceability is lacking-there is no reference to calibrated instruments, measurement standards, or SI-traceable procedures. Similarly, the study does not report any measurement uncertainty. Overall, the study's emphasis is on practical system performance rather than metrological analysis.

C. Case Study 3: QKD-TFD Integration on the NQL

The paper [9] presents a dual-purpose optical fiber infrastructure for both time and frequency dissemination (TFD) and QKD over an 78 km segment of the Niedersachsen Quantum Link (NQL), using separate fibers for each function. Link attenuation was $\sim$ 25 dB, characterized with an industrial OTDR and cross-validated using OPMs in both field and laboratory environments. Polarization-entangled photon pairs were generated via spontaneous parametric down-conversion in ppKTP crystals, pumped by a 532 nm laser. Detection was performed using SPADs at Alice and SNSPDs at Bob. The system achieved a QBER of 3% and a SKR of up to 30 bits/s over 102 km. Background photon rates due to Raman scattering were measured with SNSPDs, revealing levels around 10^{10} cps in the 10 nm QKD passband. Polarization control is achieved without direct SOP measurement by exploiting the use of a Faraday mirror, which passively compensates for polarization fluctuations in the fibre link. Synchronization was achieved using the *ELectronic STABilization (ELSTAB)* system, a commercial unit (OSTT-4L by PIKTime Systems [34]), which provides a time uncertainty of approximately 3 ps (1 PPS) over a 10 s averaging period and a frequency uncertainty below 3×10^{-13} at 1 s for a 10 MHz signal. Delay fluctuations were actively compensated. System performance was validated using a K+K FXE frequency counter (FXE-19 by K+K Messtechnik [35]), with a phase uncertainty of 12.2 ps and a frequency uncertainty of 1.2×10^{-11} at 1 s. The system achieved fractional frequency instability as low as 1×10^{-21} at 10^5 s averaging, it means the system's frequency changes almost not at all. Environmental influences were modeled rather than directly sensed, using Python-based simulations and veri-

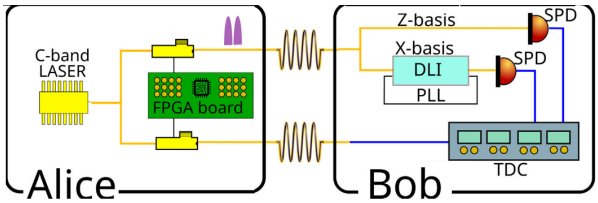

Fig. 2. A schematic of the QKD implementation, including the transmitter-receiver setup and synchronization [11].

Case Study	Key Attributes	Achievements	Limitations
Case 1 [33] Room-Temp QKD	QBER $3.4\% \pm 0.2\%$ (Type A); Channel loss $30\% \pm 2\%$ (Type B); DCR $\sim 10^{-6}$ cps (Type A)	SKR 0.5 ± 0.05 Mbits/s (Type A, B); Room-temp source; calibrated optical loss meaurements; defined uncertainties; traceable measurements	Lab-only; manual alignment limits reproducibility
Case 2 [8] 78 km Fiber QKD	26-29 dB loss (OTDR); SPAD + SNSPD detection; QBER 11%; DCR 5000 cps	Field deployment; SKR up to 1200 bps; 24-hr stability	No uncertainty or calibration traceability
Case 3 [9] QKD-TFD on NQL	$\sim$ 25 dB loss; QBER 3%; ELSTAB sync $\sim$ 3 ps uncertainty	Integrated QKD and TFD; SKR up to 30 bps; frequency instability $\sim 10^{-21}$	No uncertainty budget or traceability; polarization control indirect; environmental effects modeled
Case 4 [11] Inter-EU QKD Network	Link loss 14–25 dB; SPDs with 20% efficiency, DCR $\sim 2.5kcps$; QBER 0.82-7%; 1 ps timing resolution	SKR up to 3130 bps; stable 7-hr operation; some reproducibility across three field links	No uncertainty or polarization analysis; limited calibration details

Table 1. Concise metrological comparison of the case studies of QKD implementations.

fied via filtered SNSPD measurements [9]. This paper investigates critical elements of quantum channel characterization. Although the consistency between laboratory and field measurements demonstrates repeatability, the lack of traceability, standardized calibration procedures, and comprehensive uncertainty budgets constrains the overall metrological reliability of the results.

D. Case Study 4: The Inter-European QKD Network

The paper [11] describes a real-world deployment of a QKD network linking Italy, Slovenia, and Croatia via fiber optics, as shown in Fig. 2. Pulses were generated using a C-band laser. The system employed SPDs from ID Quantique, MPD, and Aurea, with a detection efficiency of 20% and a count rate in the range of 2500 cps. However, the detectors experienced dark counts of approximately 2.5 kcps. Timestamping was performed using TDCs from Qutools (QuTAG) and Swabian Instruments (Ultra), offering picosecond-level precision with 1 ps resolution. Synchronization was implemented using an intensity modulator controlled by an FPGA, in combination with TDCs, achieving timing accuracy better than one trillionth of a second. A Delay-Line Interferometer (DLI) was used to compare two time-separated light pulses and measure their phase difference. Combined with a PLL, it enabled phase adjustment through a feedback loop. Channel attenuation was estimated based on power loss across the fiber links, with reported values of 14 dB for the Trieste–Postojna and Ljubljana–Postojna links, and 25 dB for the Trieste–Rijeka link. SKRs reached up to 3130 bps, and QBERs ranged from 0.82–2.9% in the Z-basis and up to 7% in the X-basis. While dark counts were monitored, no calibration method was described, and polarization drift was not addressed. Environmental effects were mitigated using adaptive temporal filters (60–200 ps), which improved signal quality despite the absence of calibrated sensors From a metrological perspective, the study demonstrated good repeatability—evident in stable 7-hour operation—and some level of reproducibility across three field links with different configurations.

V. DISCUSSION AND RESEARCH GAPS

A comparative evaluation of the selected QKD implementations (Case Studies 1–4) highlights notable differences in how metrological principles are integrated into both experimental and field deployments. As summarized in Table 1, only Case Study 1 [33] provides a comprehensive metrological treatment including traceability, quantified uncertainties, and reproducibility under laboratory conditions. Case Study 1 demonstrates the most important metrological approach, incorporating both Type A and Type B uncertainty evaluations for critical parameters such as optical loss (reported as $30\% \pm 2\%$), QBER ($3.4\% \pm 0.2\%$), and SKR (0.5 ± 0.05 Mbps). The use of calibrated power meters and explicit uncertainty reporting establishes a traceable measurement foundation. However, its applicability is limited by the laboratory setting and manual alignment that restrict reproducibility. In contrast, Case Studies 2 [8], 3 [9], and 4 [11] emphasize practical system deployment, synchronization advances, and environmental integration but largely omit formal uncertainty quantification and traceability. For example, Case Study 2 reports fiber attenuation via OTDR (up to 29 dB) and SKR values (up to 1200 bps) without uncertainty budgets or calibration traceability. Similarly, Case Study 3 achieves sub-picosecond synchronization and frequency stability down to 10^{-21} but does not provide an uncertainty budget for QKD parameters nor direct SOP measurement. Case Study 4 demonstrates multi-country QKD operation with SKRs up to 3130 bps and timing resolution at the picosecond scale, yet lacks calibration details and uncertainty evaluation, especially regarding polarization effects.

From a metrological perspective, the following research gaps are evident: (I) *Traceability:* Most field-deployed systems lack references to SI-traceable standards or national metrology institutes, limiting confidence in measurement comparability. (II) *Uncertainty Quantification:* Formal error analyses and uncertainty budgets are generally absent, undermining the reliability of reported QKD performance metrics. (III) *Reproducibility:* While some temporal repeatability is documented (e.g., 24-hour stability in Case Study 2, 7-hour operation in Case Study 4), cross-system or cross-site reproducibility through independent validations or round-robin tests remains unaddressed. (IV) *Environmental Effects:* Temperature, vibration, and other environmental disturbances are acknowledged but not systematically modeled or incorporated into uncer-

tainty estimates, particularly in field conditions. (V) *Standardized Synchronization:* Timing and frequency synchronization methods are often undocumented without benchmarking against established metrological references, despite their critical role in minimizing QBER.

Bridging the gap between quantum communication engineering and metrology is essential to support reliable deployment and certification of QKD systems. Future research should prioritize integrating SI-traceable instruments, adopting uncertainty evaluation protocols consistent with the *Guide to the Expression of Uncertainty in Measurement* (GUM) [36], and developing standardized test procedures to ensure interoperability and comparability across QKD platforms.

VI. CONCLUSION

This paper examined QKD from a metrological perspective, highlighting the importance of traceability, repeatability, and uncertainty analysis in the characterization of key quantum channel parameters, including channel loss, DCR, QBER, SKR, and synchronization. To support this analysis, real-world case studies are examined. The detailed case studies showed that laboratory experiments tend to address metrological considerations more than field implementations. Notably, significant shortcomings were identified in the standardization of measurement practices, particularly in field settings where environmental effects introduce substantial measurement uncertainty and reduce comparability across systems.

REFERENCES

[1] Y.Cao, Y.Zhao, Q.Wang, J.Zhang, S.X.Ng, and L.Hanzo. The evolution of quantum key distribution networks: On the road to the qinternet. *IEEE Communications Surveys & Tutorials*, 24(2):839–894, 2022.

[2] P.Sharma, A.Agrawal, V.Bhatia, S.Prakash, and A.K.Mishra. Quantum key distribution secured optical networks: A survey. *IEEE Open Journal of the Communications Society*, 2:2049–2083, 2021.

[3] R.Steijl. Quantum information science-recent advances and computational science applications.

[4] BIPM, IEC, IFCC, ILAC, ISO, IUPAC, IUPAP, and OIML. International Vocabulary of Metrology — Basic and general concepts and associated terms (VIM). Joint Committee for Guides in Metrology, JCGM 200:2012. (3rd edition).

[5] B.Zhao, X.Zha, Z.Chen, R.Shi, D.Wang, T.Peng, and L.Yan. Performance analysis of quantum key distribution technology for power business. *Applied Sciences*, 10(8):2906, 2020.

[6] VIAVI Solutions Inc. What is an optical power meter?, n.d. Accessed: 2025-08-05.

[7] SISCO. What is an optical time domain reflectometer and how does it work?, n.d. Accessed: 2025-08-05.

[8] A.Hreibi, A.K.Kniggendorf, A.Kuhl, J.Kronjäger, H.Schnatz, and S.Kück. Entanglement-based intercity quantum key distribution: metrology and implementation. *Measurement: Sensors*, page 101777, 2025.

[9] A.K.Kniggendorf, A.Hreibi, J.Kronjäger, and S.Kück. Time and frequency dissemination and quantum key distribution on the niedersachsen quantum link–a practical approach. *Measurement: Sensors*, page 101776, 2025.

[10] G.Q.Ramzi and A.I.Khaleel. Performance evaluation of underwater bb84 protocol using various single photon counting modules. *Journal of Optics*, pages 1–9, 2025.

[11] D.Ribezzo, M.Zahidy, I.Vagniluca, N.Biagi, S.Francesconi, T.Occhipinti, L.K.Oxenløwe, M.Lončarić, I.Cvitić, M.Stipčević, et al. Deploying an inter-european quantum network. *Advanced Quantum Technologies*, 6(2):2200061, 2023.

[12] R.Nock, N.Dahnoun, and J.Rarity. Low cost timing interval analyzers for quantum key distribution. In *2011 IEEE international instrumentation and measurement technology conference*, pages 1–5. IEEE, 2011.

[13] L.Bacsardi, A.Mihaly, and K.Olah. From free-space quantum communication systems to satellite-based networks. In *2025 International Conference on Quantum Communications, Networking, and Computing (QCNC)*, pages 100–104. IEEE, 2025.

[14] D.Bolotov, M.Kuzmin, A.Nasaraia, N.Pchelkina, and S.Kuznetsov. A method for estimating losses in a quantum channel for implementing quantum key distribution technology for atmospheric laser communication terminals. In *2022 Wave Electronics and its Application in Information and Telecommunication Systems (WECONF)*, pages 1–5. IEEE, 2022.

[15] G.Keiser. *Fiber Optic Communication Networks*, pages 507–575. Springer Singapore, Singapore, 2021.

[16] Losses in optical fiber. `https://www.scribd.com/document/485321971/Losses-in-optical-fiber`. Accessed: 2025-07-21.

[17] P.Kumar and A.Prabhakar. Bit error rates in a frequency coded quantum key distribution system. *Optics Communications*, 282(18):3827–3833, 2009.

[18] N.J.Muga, M.F.S.Ferreira, and A.N.Pinto. Qber estimation in qkd systems with polarization encoding. *Journal of Lightwave Technology*, 29(3):355–361, 2011.

[19] G.Bebrov. On the (relation between) efficiency and secret key rate of qkd. *Scientific Reports*, 14(1):3638, 2024.

[20] M.Rahmanpour, M.Khaje, A.Erfanian, M.Fahimifar, and A.Afifi. Afterpulse and dark count simulator for single photon avalanche detector. 2023.

[21] M.Li, N.Rodphai, C.Liu, Z.Wang, Z.Peng, J.Wang, N.Anfimov, D.Korablev, T.Lachenmaier, A.G.Olshevskiy, et al. Dark count rate stability of juno 20-inch pmts in mass testing. *arXiv preprint arXiv:2506.15164*, 2025.

[22] O.Bedroya, C.Li, W.Wang, J.Hu, H.Lo, and L.Qian. Resource-efficient real-time polarization compensation for mdi-qkd with rejected data. *Quantum*, 8:1435, 2024.

[23] V.Mayboroda, N.Rudavin, P.Kupriyanov, O.Fat'yanov, and R.Shakhovoy. Analytical solution to the problem of polarization drift compensation in an all-fiber qkd system. *Optics Express*, 32(26):45421–45435, 2024.

[24] R.D.Cochran and D.J.Gauthier. Qubit-based clock synchronization for qkd systems using a bayesian approach. *Entropy*, 23(8):988, 2021.

[25] A.Pljonkin, K.Rumyantsev, and P.Kumar Singh. Synchronization in quantum key distribution systems. *Cryptography*, 1(3):18, 2017.

[26] A.Czerwinski and S.Haddadi. Optimizing qkd efficiency by addressing chromatic dispersion and time measurement uncertainty. *Physics Letters A*, 526:129972, 2024.

[27] N.Chandra and P.K.Krishnamurthy. Fpga based synchronization of frequency domain interferometer for qkd. *IEEE Transactions on Quantum Engineering*, 2024.

[28] G.Granados, W.Velasquez, R.Cajo, and M.Antonieta-Alvarez. Quantum key distribution in multiple fiber networks and its application in urban communications: A comprehensive review. *IEEE Access*, 2025.

[29] M.A.Butt, G.S.Voronkov, E.P.Grakhova, R.V.Kutluyarov, N.L.Kazanskiy, and S.N.Khonina. Environmental monitoring: A comprehensive review on optical waveguide and fiber-based sensors. *Biosensors*, 12(11):1038, 2022.

[30] Y.Lei, R.Li, L.Zhang, P.Hu, and Q.Huang. Optical accelerometers for detecting low-frequency micro-vibrations. *Applied Sciences*, 12(8):3994, 2022.

[31] A.Theodosiou. Recent advances in fiber bragg grating sensing. *Sensors*, 24(2):532, 2024.

[32] C.Xu, X.Hao, P.Pei, T.Wei, and S.Feng. Research on time constant test of thermocouples based on qnn-pid controller. *Sensors*, 25(12):3819, 2025.

[33] G.Murtaza, M.Colautti, M.Hilke, P.Lombardi, F.S.Cataliotti, A.Zavatta, D.Bacco, and C.Toninelli. Efficient room-temperature molecular single-photon sources for quantum key distribution. *Opt. Express*, 31(6):9437–9447, Mar 2023.

[34] Ostt-4 fiber-optic. `https://piktime.com/offer/ostt-4/`, 2025. Accessed: 2025-08-01.

[35] K+k messtechnik gmbh. `https://kplusk-messtechnik.de/`, 2025. Accessed: 2025-08-01.

[36] JCGM. Guide to the expression of uncertainty in measurement, 1995. JCGM 100:2008 (corrected version of first edition 1995).